Prospects for the measurement of m_W at the LHC

M. Boonekamp

CEA / IRFU,

91191 Gif-sur-Yvette, France

I describe the status of the m_W measurement preparations in ATLAS and CMS, with particular focus on the uncertainties induced by the strong interaction.

1 Relevance of the W boson mass and principle of its measurement

The Standard Model (SM) [1,2,3] including radiative corrections [4] provides a predictive theoretical framework in which the fundamental parameters (particle masses and couplings) are interconnected *via* an overconstrained set of relations. This can be exploited to test the validity of the SM. With precisely known Z boson mass (m_Z), Fermi coupling parameter (G_F), electromagnetic and strong coupling constants ($\alpha_{\mathrm{QED}}, \alpha_{\mathrm{S}}$) and electroweak mixing angle $\sin^2 \theta_W$, currently the most interesting set of constraints relates the Higgs boson mass m_H to m_W and to the top quark mass m_{t}. The curve correlating m_W and m_{t} is a definite prediction for any given m_H. Comparison with the actual measured values of m_W and m_{t} constitutes a test of this prediction.

This discussion is illustrated in Figure 1, which reports m_W as a function of m_{t} for various Higgs boson mass hypotheses [5]. The central curve corresponds to $m_H = 125.7 \pm 0.4$ GeV. The data point represents the current measured values $m_W = 80.385 \pm 0.015$ GeV and $m_{\mathrm{t}} = 173.2 \pm 0.9$ GeV. It can be seen from this figure the uncertainty on m_W currently drives the compatibility of the data with the prediction.

Quantitatively, when testing the validity of the SM, a top quark mass uncertainty of $\delta m_{\mathrm{t}} = 0.9$ GeV is matched in sensitivity by $\delta m_W \sim 6$ MeV, *i.e.* a natural obective for the W boson mass accuracy is an improvement by a factor 2.5 to 3 compared to present knowledge. Achieving this goal constitutes a test of the SM by itself; further improvement in δm_{t} will become relevant on that timescale.

The measurement relies on the assumption that the kinematic peaks of the W boson decay products (p_T^l, p_T^ν, m_T) can be predicted accurately for a given hypothesis for m_W. To this end, physics generators are used to describe the production and decay process, and realistic distributions are obtained using detector simulation. The detector-level decay product distributions, or template distributions, are then constructed for a set of reasonable m_W hypotheses by varying the mass parameter in the generator. All templates are compared to the data and the best match is determined. Likely the simplest possible measurement from the statistical point of view, the difficulty lies of course in the construction of the templates. These carry physics and experimental uncertainties that need to be evaluated and constrained, as summarized in the next section.
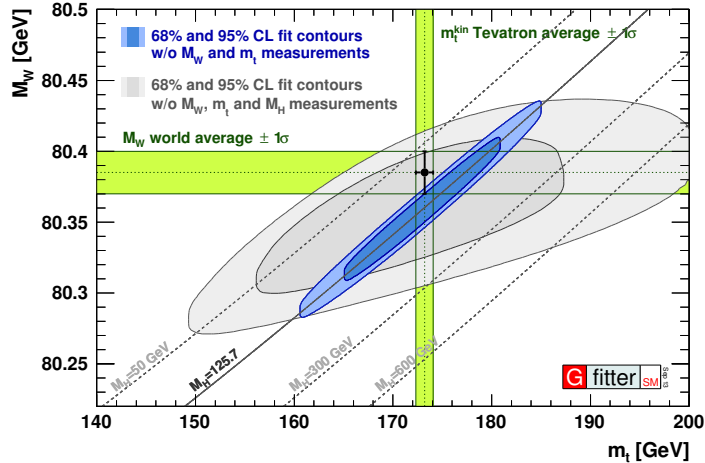
Figure 1 – Comparison of the measured W boson and top quark masses with their predicted values in the Standard Model.

2 Challenges

In contrast to for example the Z boson mass measurement at LEP, or the measurement of $\sin^2 \theta_W$ at SLC, where the main requirements were excellent theoretical and experimental control of the initial state, these measurements at hadron colliders almost entirely rely on the understanding of the final state. That is, in the processes

$$pp \to Z + X \to ll + X,$$

$$pp \to W + X \to l\nu + X,$$

the fundamental parameters are extracted from the final state kinematic peaks, as explained in the previous section: the dilepton invariant mass $M(ll)$, the Jacobian peaks of p_T^l, p_T^ν and the transverse mass $m_T = (p_T^l p_T^\nu (1 - \cos \Delta\phi))^{1/2}$, as well as the asymmetries $A_{FB} = (\sigma_F - \sigma_B)/(\sigma_F + \sigma_B)$. The observed distributions of these observables however reflect a combination of experimental and physics effects that need to be disentangled before attempting a physical interpretation. I summarize the main steps below.

The first major goal is a control of the ATLAS and CMS detector energy and momentum scales. These simple final states are dominated by the W or Z decay leptons; the rest of the event, consisting of mostly soft hadronic activity, is considered as a global quantity recoiling against the decaying boson.

In the muon channel, low-mass vector mesons (J/ψ, Υ), W and Z bosons are collected in approximate 10:10:1 proportions, while the relative uncertainties on their masses are $\sim 10^{-6}$, $\sim 10^{-4}$, $\sim 10^{-5}$ respectively. This suggests to use J/ψ and Z events to constrain the momentum scale; the muon calibrations can be applied to the measurement of m_W. In the electron channel, J/ψ events are not collected as efficiently, so that the Z sample constitutes the main handle on the EM calorimeter energy scale. In the case of electrons, a major difficulty is to understand the calorimeter intercalibration, and the passive detector material upstream of it, before the $Z \to ee$ peak position can reliably be interpreted in terms of the calorimeter energy scale and used as a reference applying to W production. The hadronic recoil, input to the calculation of the missing transverse energy $E_T(\nu)$ and m_T, is calibrated exploiting momentum balance in Z events (after lepton calibration).

After the completion of the LHC Run 1, the LHC detectors have finalized their calibrations and published an extensive set of results on electron, muon and recoil performance [6,7,8]. Thanks to the large collected samples, the quality of the modeling of the data by the simulation has been vastly improved compared to initial performance. The J/ψ, v and Z leptonic decay samples play a particular rôle in this context as the precisely known mass of these particles constrains the absolute scale of the detectors. In addition, since the decay is fully measured, momentum balance in the transverse plane can be exploited to determine the response and resolution of the hadronic recoil. Two example performance plots are are shown in Figure 2. In the following it will be assumed that the understanding of the detector performance is adequate for a measurement of m_W, and these aspects will not be discussed further.
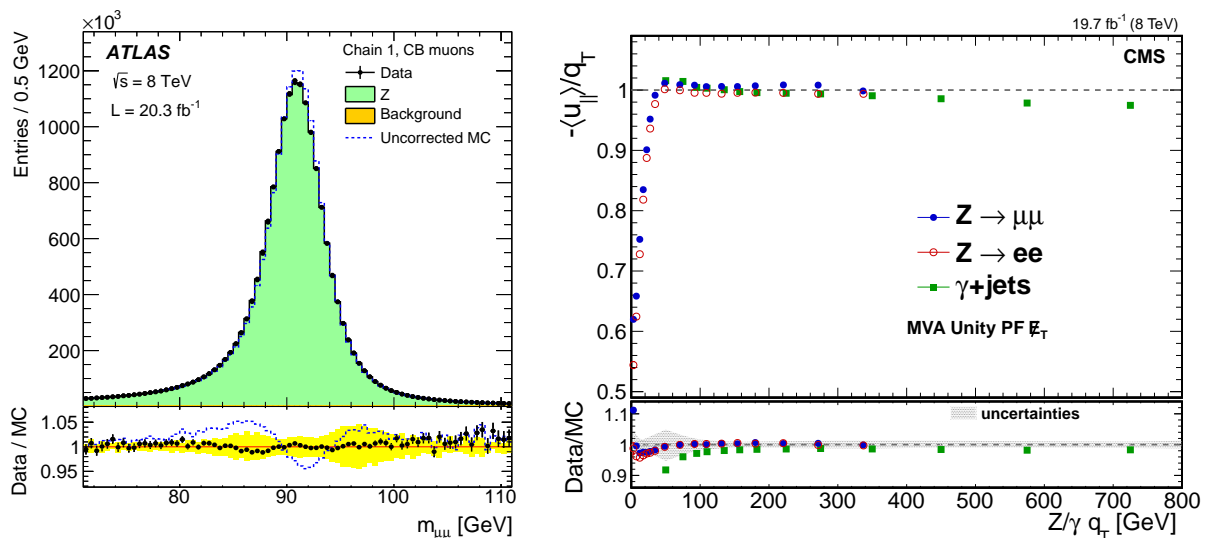

Figure 2 – Left: muon pair invariant mass distribution in the Z peak region, in ATLAS. Right: performance of recoil reconstruction in Z eventsm in CMS.

Complications in the physics modeling of W and Z production originate from strong interaction effects. The proton parton density functions (PDFs) and the initial-state interactions of the colliding partons determine the production distributions, and are partly governed by non-perturbative mechanisms that can not be entirely predicted from first principles.

The W and Z production data themselves are used to specify the models. The most relevant proton PDF constraints are obtained from measurements of the inclusive W^+, W^- and Z production rates and rapidity distributions. These observables and their ratios allow, together with slightly more complex final states such $W + c$ and $\gamma + c$, a full flavour decomposition of the proton PDFs and a mapping of their Bjorken x dependence.

When colliding, the initial state partons radiate a large number of mostly soft gluons, as a result of their mutual interactions. This initial state "parton shower" contributes to the transverse momentum distribution of the W and Z. The details of this process are not fully predictible and are modeled in a semi-phenomenological way; the Z sample provides the main handle to constrain the model parameters.

In contrast, electroweak corrections to these processes, mostly inherited from the LEP/SLC era, are accurately known, need to be properly taken into account (using appropriate programs) but do not constitute a major source of uncertainty.

3 W boson production and decay

In order to interpret the kinematic peaks of the W decay products as probes of m_W, other effects influencing these distributions must be understood to high accuracy. To be specific: the distribution of $p_T(l)$ reflects, in addition to m_W, the W boson rapidity and transverse momentum distributions and the angular distributions of the decay products, i.e. the W polarization. These in turn largely result from the partonic sub-process, which receives significant contributions from first and second generation quarks. I discuss two specific examples below, to highlight the preparatory role of vector boson production measurements.

W polarization from the valence quark distributions

Consider the decay of a W^+ boson produced at y_W and with $p_T(W) = 0$, so its polarization is purely transverse. The momentum fractions of the partons involved in the process are

$$x_1 = \frac{m_W}{\sqrt{s}} e^{y_W} \quad ; \quad x_2 = \frac{m_W}{\sqrt{s}} e^{-y_W}$$

where $x_1 > x_2$ is assumed, and the parton of highest momentum is oriented towards $z > 0$. Considering first generation quarks only, the relevant sub-process is $u\bar{d} \to W^+$. The cross section receives contributions from u quarks oriented towards $z > 0$ and $z < 0$:

$$\left.\frac{\partial\sigma}{\partial y}\right|_{z>0} \propto u_1 \bar{d}_2 \quad ; \quad \left.\frac{\partial\sigma}{\partial y}\right|_{z<0} \propto u_2 \bar{d}_1$$

where we use the shorthand $u_i \equiv u(x_i)$ and similarly for $\bar{d}$, and $u(x), \bar{d}(x)$ are the up and anti-down quark densities in the proton at momentum fraction x. The first term corresponds to the W being boosted in the direction of the incoming valence quark, and dominates. Introducing θ^*, the angle between the decay lepton and the oriented z axis, the cross section writes

$$\begin{aligned}
\frac{\partial^2\sigma}{\partial y\, \partial\cos\theta^*} &\propto u_1\bar{d}_2(1-\cos\theta^*)^2 + u_2\bar{d}_1(1+\cos\theta^*)^2 \\
&= (u_1\bar{d}_2 + u_2\bar{d}_1)(1+\cos^2\theta^*) - 2(u_1\bar{d}_2 - u_2\bar{d}_1)\cos\theta^*
\end{aligned}$$

The first term is even in θ^* and unpolarized. Defining the valence and sea distributions as $u_V(x) = u(x) - \bar{u}(x)$ and $\bar{u}(x) = \bar{d}(x) = q(x)$, the second term becomes

$$(u_1\bar{d}_2 - u_2\bar{d}_1)\cos\theta^* \propto (u_{V1}q_2 - u_{V2}q_1)\cos\theta^* \sim u_{V1}q_2\cos\theta^* \tag{1}$$

for sufficiently large y_W, since when $x_1 \gg x_2$, $u_{V1} \gg u_{V2}$ and $q_1 \ll q_2$. The overall cross section thus deviates from the unpolarized $(1 + \cos^2\theta^*)$ distribution by an amount proportional to the valence distribution. The polarized term disappears when $y_W = 0$, as $x_1 = x_2$ and $(u_{V1}q_2 - u_{V2}q_1) = 0$ whatever the valence distribution. Due to the undetected neutrino, this configuration can however not be isolated in the experiment. The impact of this residual polarization on the $p_T(l)$ distribution is illustrated in Figure 3-a, taken from [9], where the natural distribution is compared to the unpolarized distribution obtained in the hypothetical case where $u_V = 0$. Similar arguments hold for the W^- and involving the d-quark valence, d_V.

The strange density and the charm quark mass

In $cs \to W$ events, the c quark entering the collision has on average higher transverse momentum that the light quarks. This is due to the usual threshold suppression factor present in the $g \to c\bar{c}$ splitting function, at gluon virtuality Q^2, which favours $Q >> 2m_c$, giving more phase space and inducing higher transverse momentum on average compared to light quark splitting functions.
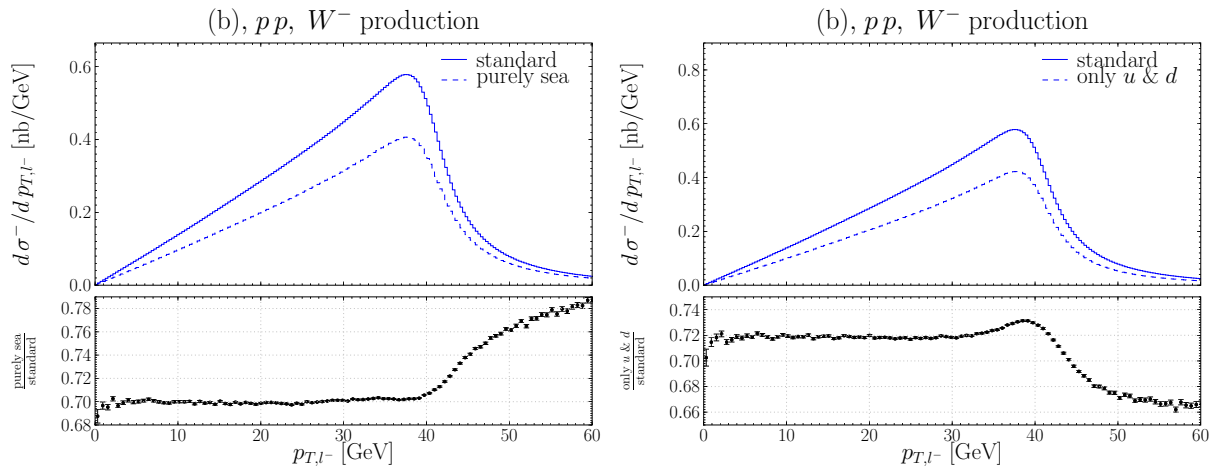
Figure 3 – Left: lepton transverse momentum distributions in W decays, with and without valence contributions. Right: lepton transverse momentum distributions in W decays, with and without contributions from second generation quarks.

As a result, generators predict that $p_T(W)$ is harder in $cs \to W$ events compared to $ud \to W$, by an amount of order m_c. Consequently, the p_T^l distributions differ for these two processes, reflecting a convolution with different underlying $p_T(W)$ distributions. Figure 3-b illustrates the effect, comparing the $p_T(l)$ distributions for the natural mix of sub-processes with that obtained for $ud \to W$ only. A proper modeling of the p_T^l distribution thus relies on our evolving knowledge of the strange density and of the non-perturbative parameters which together determine the p_T^W distribution.

4 Experimental constraints

The LHC experiments have engaged in an extensive measurement program that aims at constraining the QCD parameters describing these effects. Strong experimental constraints on the PDFs come from the W cross sections, measured differentially in lepton pseudorapidity; in particular the eta-dependent W charge asymmetry is specifically sensitive to the u and d valence ratio. These measurements have been pursued by ATLAS and CMS [10]. Z cross section measurements are also performed [11,12]; in conjunction with the W cross section, this provides information on the strange density [13]. The strange density can also be probed directly, via measurements of $W + c$ production [14]. The non-perturbative parameters are most accurately probed through measurements of the Z boson transverse momentum measurements [15], or of the angular correlations of its decay products [16]. Figure 4 illustrates two selected results.

While the existing body of measurements is impressive, the available data are far from fully exploited. In particular, inclusive W production at 8 TeV has not been studied and is important to pursue. Needless to say, the forthcoming Run 2 data, taken at much higher centre-0f-mass energy, will provide extremely useful and complementary information. At $\sqrt{s} \sim 13$ TeV, the typical parton momentum fraction probed is lower than in Run 1, enhancing the influence of the proton sea, and allowing further constraints in this region.

5 Perspectives

The LHC experiments are reaching maturity in terms of detector understanding, and have performed a wide range of measurements aimed at a better understanding of the the proton structure and the strong interaction. A large W sample is also available, sufficient to reach a
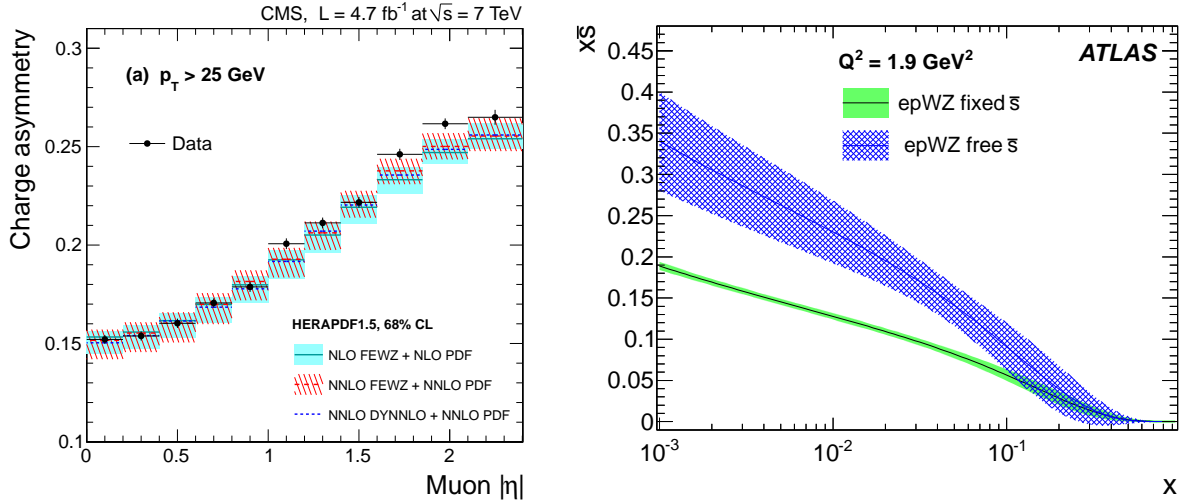
Figure 4 – Left: lepton charge asymmetry at 8 TeV, measured by CMS. Right: strange density determined from the W and Z inclusive cross sections at 7 TeV, from ATLAS.

2 MeV statistical sensitivity on a measurement of m_W.

To complete the first measurements of m_W still requires to combine all the available information in a consistent way. The measured cross sections and rapidity and transverse momentum distributions should be exploited to constrain the proton PDFs and the non-perturbative resummation parameters, properly accounting for the physical correlations between these effects. Such an analysis has not been performed before and is a requirement for a successful measurement of m_W.

References

1. S. L. Glashow, Nucl. Phys. **22**, 579 (1961).
2. A. Salam, Conf. Proc. C **680519** (1968) 367.
3. S. Weinberg, Phys. Rev. Lett. **19**, 1264 (1967).
4. D. Y. Bardin, P. Christova, M. Jack, L. Kalinovskaya, A. Olchevski, S. Riemann, and T. Riemann, *Comput. Phys. Commun.* **133**, 229 (2001).
5. M. Baak, M. Goebel, J. Haller, A. Hoecker, D. Kennedy, R. Kogler, K. Moenig and M. Schott *et al.*, Eur. Phys. J. C **72**, 2205 (2012).
6. G. Aad *et al.* [ATLAS Collaboration], Eur. Phys. J. C **74**, no. 11, 3130 (2014).
7. V. Khachatryan *et al.* [CMS Collaboration], JINST **10**, no. 02, P02006 (2015).
8. G. Aad *et al.* [ATLAS Collaboration], Eur. Phys. J. C **72**, 1844 (2012).
9. M. W. Krasny, F. Dydak, F. Fayette, W. Placzek and A. Siodmok, Eur. Phys. J. C **69**, 379 (2010).
10. S. Chatrchyan *et al.* [CMS Collaboration], Phys. Rev. D **90**, no. 3, 032004 (2014).
11. V. Khachatryan *et al.* [CMS Collaboration], arXiv:1504.03511 [hep-ex].
12. G. Aad *et al.* [ATLAS Collaboration], Phys. Rev. D **85**, 072004 (2012).
13. G. Aad *et al.* [ATLAS Collaboration], Phys. Rev. Lett. **109**, 012001 (2012).
14. S. Chatrchyan *et al.* [CMS Collaboration], JHEP **1402**, 013 (2014).
15. G. Aad *et al.* [ATLAS Collaboration], Phys. Lett. B **738**, 25 (2014).
16. G. Aad *et al.* [ATLAS Collaboration], Phys. Lett. B **720**, 32 (2013).